

NONEQUILIBRIUM BOUND INTERFACES

F. de los Santos¹ and M.M. Telo da Gama²

¹Departamento de Electromagnetismo y Física de la Materia,
Universidad de Granada, Fuentenueva s/n, 18071 Granada,
Spain

²Centro de Física Teórica e Computacional e
Departamento de Física da Faculdade de Ciências da
Universidade de Lisboa, Av. Prof. Gama Pinto, 2, P-1643-003
Lisboa Codex, Portugal

Abstract

An overview of recent studies of nonequilibrium bound interfaces is given. Attention is focused on Kardar-Parisi-Zhang interfaces in the presence of upper and lower walls, interacting via short- and long-ranged potentials. A comparison with equilibrium interfaces is carried out, and connections with other nonequilibrium systems are illustrated. Experimental realizations of the phenomenology described in this article are briefly discussed.

1 Introduction

An interface is the moving or static boundary between two distinct bulk phases. Effective descriptions that focus on the statistical properties of the interfacial degrees of freedom have proved particularly useful, and over the past decades received a great deal of attention [1, 2, 3, 4]. Within this approach, the essence of the bulk contributions is incorporated into the (continuous or discrete) model parameters; other effects, such as geometric constraints, are modeled as nontrivial surface terms. Examples of the latter abound, and include the morphology and motion of an interface constrained by the presence of a third phase, by an external field, by inhomogeneities of

the medium, etc. In thermal equilibrium, or near equilibrium, enormous theoretical, as well as experimental, progress was made. For example, wetting in the two-dimensional Ising model was shown to be uniquely described by an interfacial model on sufficiently large length scales [5]. Of more practical interest are three-dimensional systems with realistic interactions, for which a number of theoretical predictions have been confirmed experimentally [6]. However, for nonequilibrium systems this field of research is only just starting.

In this review, we give an overview of recent theoretical results on nonequilibrium bound interfaces. The focus will be on a few models, mostly in the form of continuum stochastic growth equations, that are expected to be representative of a broad class of physical phenomena. The primary reason for this choice is that, the statistical properties being identical to those of the discrete models, continuum equations are more adequate to describe the collective behavior at the macroscopic level, and thus give a unified picture of the field. Although the discussion is intended to be general, unless otherwise stated, results pertaining to one-dimensional systems only are given.

This paper is organized as follows. Firstly, in Section 2 a brief discussion of the kinetics of two representative, free-interface models is provided. In Section 3, we review the implications brought about by the inclusion of interacting, binding walls. Next, we explore analogous phenomena in other systems and in the last section describe experimental systems where bound-KPZ behavior could be observed. Much of this material has been covered from a different perspective in a recent review [7].

2 Two models of free interfaces

2.1 The Edwards-Wilkinson equation

The following Langevin equation, referred to as the Edwards-Wilkinson equation, is commonly employed to describe on a coarse-grained level the dynamics of an interface separating two bulk fluid phases [8],

$$\frac{\partial h(\mathbf{x}, t)}{\partial t} = \nu \nabla^2 h + \eta(\mathbf{x}, t), \quad (1)$$

where $h(\mathbf{x}, t)$ is the local height of the interface above some reference plane. ν is the interfacial tension or the interfacial stiffness if any of the coexisting

phases is anisotropic. It measures the strength of the Laplacian, a relaxing term that arises from bulk evaporation-condensation processes. Microscopic fluctuations, which in the present case are assumed to have a thermal origin, are modeled by the stochastic noise term $\langle \eta \rangle$, with mean $\langle \eta \rangle = 0$ and variance $\langle \eta(\mathbf{x}, t) \eta(\mathbf{x}', t') \rangle = 2D\delta(t-t')\delta(\mathbf{x}-\mathbf{x}')$, where $\langle \cdot \rangle$ denotes an average over the noise distribution. Since the system is in thermal equilibrium, the noise correlation function is related to the temperature through the fluctuation-dissipation theorem, i.e. $D = k_B T$. Finally, note that this model ignores configurations containing overhangs and bubbles, as $h(\mathbf{x}, t)$ is a single-valued function.

An interface governed by the EW equation does not move on average irrespective of its initial position. This agrees with the thermodynamic picture that at bulk coexistence any arbitrary fraction of the system may be in one phase, with the remainder in the other. Adding a constant μ to (1) drives the system out of coexistence. For instance, if $\mu > 0$ the steady-state interface moves upwards with an average velocity $v = \mu$, thereby favoring the $y < h(\mathbf{x})$ phase over the unstable $y > h(\mathbf{x})$ one. In this context, μ may be interpreted as an external force acting on the interface or as the chemical potential difference between the two phases.

The fluctuations of the interface around its equilibrium position are characterized by the interfacial width, a conventional measure of interfacial roughness, defined as

$$W^2(L, t) = \langle [h(t) - \bar{h}(t)]^2 \rangle, \quad (2)$$

where $\bar{h}(t)$ is the spatial average of $h(\mathbf{x}, t)$. An initially flat surface is essentially confined between $\bar{h}(t) - W(t)$ and $\bar{h}(t) + W(t)$, at later times. It is well-known that the behavior of W depends on the system dimensionality: for $d > 2$ the interface is said to be smooth as W converges in the limit $L, t \rightarrow \infty$. At $d = 2$ the interface is logarithmically rough,

$$W^2 \sim \begin{cases} \ln(\nu t/a), & t \ll L^z, \\ \ln(L/a), & t \gg L^z. \end{cases} \quad (3)$$

Here a is a microscopic scale of the order of the bulk correlation length and L^z defines a time scale characterized by the so-called *dynamic exponent* z . Finally, in $d < 2$ the interfacial behavior is universal and given by,

$$W \sim \begin{cases} t^\beta, & t \ll L^z, \\ L^\zeta, & t \gg L^z. \end{cases} \quad (4)$$

The initial increase of the interfacial width as a power of time is governed by the *growth exponent*, β ; this is followed by a saturation regime where the interfacial width scales as $W(L, \infty) \sim L^\zeta$. The crossover between the initial and the saturation regimes occurs when the lateral correlation length $\xi(t) \sim t^{1/z}$ is of the order of the size of the system. The *roughness exponent* ζ , is a measure of the typical transverse fluctuation W of a given interfacial segment L as given by (4). This behavior is summarized by the Family-Vicsek scaling relation $W(L, t) \sim L^\zeta f(t/L^z)$, where the scaling function f satisfies $f(u) \sim u^\beta$ for $u \ll 1$ and $f(u) = \text{const}$ for $u \gg 1$ [9]. Clearly, continuity at $t = L^z$ requires $\zeta = \beta z$. Note that in an infinite system the width does not saturate, implying that the interface is rough in the sense that it makes arbitrarily large excursions from its average position. Due to the linear character of equation (1) the exponents can be calculated in arbitrary dimension. In particular, $z = 2$, $\beta = (2 - d)/4$, and $\zeta = (2 - d)/2$.

Equation (1) can be derived by differentiating a simple Hamiltonian

$$\mathcal{H}(h) = \int_0^\infty d\mathbf{x} \left[\frac{\nu}{2} (\nabla h)^2 \right] \quad (5)$$

that is recognized as the square-gradient approximation to a surface free energy that is proportional to the total interfacial area,

$$\mathcal{F} = \nu \int d\mathbf{x} \left[1 + (\nabla h)^2 \right]^{1/2}. \quad (6)$$

The study of systems off-coexistence requires the inclusion of an additional term $\mu \int h(\mathbf{x}) d\mathbf{x}$ in (5), where μ is the chemical potential difference between the two phases. Of course, all the stationary properties of the EW interface described above can be recovered from (5) in a straightforward manner.

2.2 The Kardar-Parisi-Zhang equation

As referred previously, the velocity of an interface described by the EW equation is $v = \mu$, regardless of its initial position. At $\mu = 0$ this is equivalent to bulk phase coexistence. A natural generalization of (1) consists in assuming that v is no longer constant, but depends on the instantaneous local-slope of the interface at \mathbf{x} . Thus, substituting μ by $v(\nabla h)$ and using again the

small-slope approximation one finds¹

$$v(\nabla h) \approx v(\mathbf{0}) + \nabla v(\mathbf{0}) \cdot \nabla h + \frac{1}{2}[(\nabla h) \cdot \nabla]^2 v(\nabla h = 0). \quad (7)$$

Assuming isotropy in the sense that $\partial^2 v / \partial x_i \partial x_j \propto \delta_{ij}$, and removing the first two terms through a Galilean transformation $h(\mathbf{x}, t) \rightarrow h(\mathbf{x} + \nabla v(\mathbf{0})t, t) + v(\mathbf{0})t$, yields the celebrated Kardar-Parisi-Zhang (KPZ) equation [11],

$$\frac{\partial h(\mathbf{x}, t)}{\partial t} = \nu \nabla^2 h + \lambda (\nabla h)^2 + \eta(\mathbf{x}, t). \quad (8)$$

The only difference between the KPZ and the EW equations is the nonlinear term $\lambda(\nabla h)^2$, that is the most relevant nonequilibrium perturbation to the equilibrium EW equation and is expected to describe the scaling properties of rough surfaces growing in the absence of conservation laws. Somewhat surprisingly, experimental realizations of the KPZ behavior are far from evident in marked contrast with its presence in a variety of theoretical models. It has been argued that this may be due to the occurrence of medium-induced non-local interactions [12], and/or long instability-induced transients that mask the asymptotic KPZ scaling [13].

The Family-Vicsek scaling picture (4) of the EW equation also holds for the KPZ. It turns out that in one dimension the stationary probability distribution

$$P(h) = \exp\left(-\frac{\nu}{2D} \int (\nabla h)^2 dx\right), \quad (9)$$

which is a solution of the Fokker-Planck equation of the linear theory ($\lambda = 0$) in any dimension, is also a solution of the Fokker-Planck equation corresponding to the KPZ. Hence, the nonlinearity does not affect the steady state solution and consequently the two interfaces have the same roughness exponent $\zeta = 1/2$. The other two exponents may be obtained from the relation $z = 2 - \zeta$ [14], valid in any dimension, and from $\beta = \alpha/z$, previously derived. In dimensions $d > 1$, the scaling exponents cannot be obtained analytically, nor perturbatively. At $d > d_c = 2$, both a weak and a strong-coupling regimes occur depending on whether the value $\lambda^2 D / \nu^3$ is smaller or larger than a critical value. In the weak-coupling regime, which is unstable at the critical dimension $d_c = 2$, λ vanishes asymptotically leading to the

¹It can be shown that third and higher order terms may be neglected in the large-scale limit [10].

EW behavior $z = 2, \zeta = 0$. By contrast, the strong-coupling regime is controlled by a fixed point that is not reached by perturbation analysis. Several conjectures for the critical exponents have been put forward [1], including a recent claim of a mathematical proof [15]. Another controversial aspect of the KPZ behavior concerns the existence of the upper critical dimension. For a more elaborated discussion of these (rather technical) matters, the reader is referred to existing reviews [1, 4, 16].

The KPZ nonlinearity is related to the lateral growth that occurs when a depositing particle sticks to the first particle it encounters on the surface [1]. As a consequence, by contrast to EW-like surfaces, interfaces governed by the KPZ equation have a nonzero velocity at $\mu = 0$,

$$v = \int_0^L \langle \partial_t h \rangle d\mathbf{x} = \lambda \int_0^L \langle (\nabla h)^2 \rangle d^d x = \lambda m^2, \quad (10)$$

where m^2 is the overall quadratic slope of the interface. Since the stationary probability distribution is known in $d = 1$, $m^2 = -\partial_\gamma \ln Z$ can be computed through the simple Gaussian path integral,

$$Z = \int \mathcal{D}h \exp \left(-\gamma \int (\nabla h)^2 dx \right). \quad (11)$$

with $\gamma = \nu/2D$. Thus, $v = D\lambda/4\nu a$, which depends on the microscopic scale a and is therefore nonuniversal; however, it has a universal finite-size correction $v(L) = D\lambda/2\nu L$, a result that holds for $t \gg L^z$. See [17] for a different, more detailed derivation.

As the nonlinear term of the KPZ is purely kinetic in origin, the KPZ equation cannot be obtained by differentiation of an equilibrium Hamiltonian such as (5).² Nevertheless, it can be mapped onto a linear diffusion-equation by a simple change of variables, the so-called Cole-Hopf transformation $h(\mathbf{x}, t) = (\nu/\lambda) \ln n(\mathbf{x}, t)$, yielding

$$\frac{\partial n(\mathbf{x}, t)}{\partial t} = \nu \nabla^2 n + n\eta. \quad (12)$$

This constitutes the *directed polymer representation* of the KPZ [1]. We shall take advantage of this representation in a later section but, for now, simply point out the presence of the *multiplicative noise* term.

²It has been argued, however, that equation (8) is not correct unless $\partial_t h$ and η are projected along the normal direction, in which case a non-bound Hamiltonian exists [18].

3 Bound interfaces

Let us assume that the interfacial fluctuations are restricted by the presence of another interface, by a physical barrier, or by any other mechanism capable of confining it. We will see shortly how to incorporate this effect into a growth equation. Consider a rigid, impenetrable wall that prevents large interfacial excursions in a given direction. In this case, the interfacial width approaches a constant value, $W(L, t) \rightarrow \xi_{\perp}$, as $L, t \rightarrow \infty$ even if the free interface is rough. Therefore, a bound interface is never rough. Moreover, since the fluctuations are cutoff in a given direction, there will be an effective fluctuation-induced repulsion between the wall and the interface, leading to the possibility of interfacial pinning-depinning (or unbinding) transitions.

In the following we briefly review the behavior of a modified EW equation describing an interface bound to a wall, for which the aforementioned behavior can be worked out explicitly within the mean-field approximation [19]. The case of the bound KPZ interface will be tackled afterwards.

3.1 A bound Edwards-Wilkinson equation

Restricting the height variables in the EW equation to, for instance, positive values requires supplementing (5) with the *hard* wall condition $V(h < 0) = \infty$. This is not only inconvenient for analytical studies, but also unnecessarily limited in scope. Therefore, more general types of walls will be considered, the only requirements being the *soft* wall condition $V(h) \rightarrow \infty$ as $h \rightarrow h_{wall}$, and $V(h) \rightarrow 0$ as $h \rightarrow \infty$ with $V(h)$ differentiable. In this case, the wall interacts with the interface, in addition to cutting off some of its fluctuations. The large-scale interfacial behavior as well as the character of the unbinding transitions are not expected to change as the hard-wall is replaced by a soft-wall [19]. We therefore consider the EW growth equation in the presence of an effective interface potential $V(h)$ [20, 21]

$$\frac{\partial h(\mathbf{x}, t)}{\partial t} = \nu \nabla^2 h + \mu - \frac{\partial V}{\partial h} + \eta(\mathbf{x}, t), \quad (13)$$

where η is Gaussian white noise with the same mean and variance as in (1). The region $y > h(\mathbf{x})$ corresponds to the stable thermodynamic phase, say A , the region $y < h(\mathbf{x})$ corresponds to a second phase B that coexists with A when $\mu = 0$ and $h(\mathbf{x}, t)$ is the local height of the AB interface measured from the wall (see figure (1)).

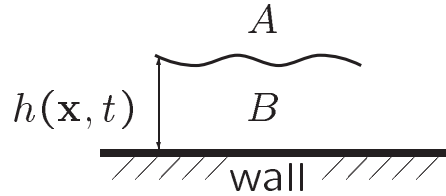


Figure 1: Separation $h(\mathbf{x}, t)$ of the AB interface from a rigid wall.

ν is the interfacial tension of the AB interface and $V(h)$ accounts for the net interaction between the interfaces binding the B layer (the *wetting* film), in this case the substrate and the AB interface. In the simple case where AB corresponds to a vapor-liquid interface, a repulsive $V(h)$ simulates adsorption of the liquid phase from the vapor. The form of $V(h)$ depends on the nature of the forces between the particles in the fluid and with the wall, and its derivation from bulk, microscopic Hamiltonians is far from trivial. Ideally one constrains the interface, away from its equilibrium flat position, in the configuration $h(\mathbf{x})$ and using the microscopic Hamiltonian, takes a partial trace over the bulk variables. Of course this cannot be done exactly for realistic Hamiltonians. In approximate derivations one usually requires consistency at the mean-field level. If all the microscopic interactions are short-ranged, one may take for sufficiently large h at bulk coexistence, [22]

$$V(h) = b(T)e^{-h} + ce^{-2h}, \quad (14)$$

where h is measured in units of the B -phase bulk correlation length, T is the temperature, $b(T)$ vanishes linearly as $T - T_w$, the wetting temperature (see below) and $c > 0$. If, instead, one considers long-ranged (van der Waals) interactions, the potential has the general form [23]

$$V(h) = b(T)h^{-m} + ch^{-n}, \quad n > m > 0, \quad (15)$$

and in this case $b(T)$ is related to the Hamaker constant. In all cases, if we add the contribution from the chemical potential difference μh to $V(h)$, the behavior of the system will be controlled by the latter term, since this is a bulk contribution that dominates over the surface term $V(h)$ except at bulk coexistence (fig. (2)). Finally, note that the present description assumes the existence of an interface and thus it is only valid below the bulk critical temperature, where distinct “liquid” and “gas” phases are defined.

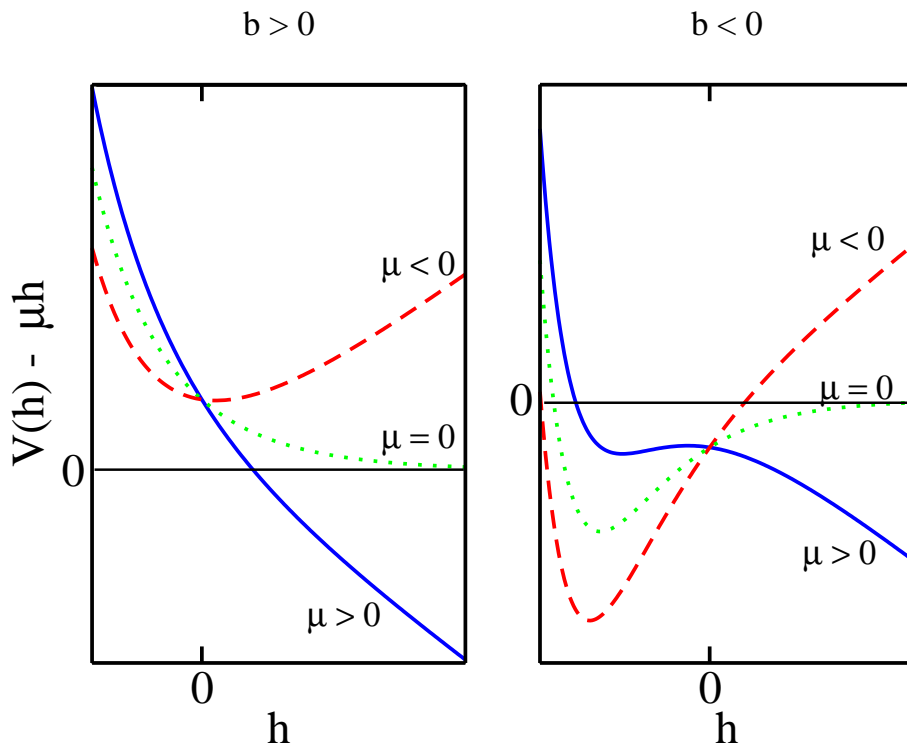


Figure 2: Typical effective interfacial potentials for negative and positive values of b . Below the transition temperature, the potential well localizes the interface (dotted lines).

Some remarks concerning the connection of equation (13) with wetting phenomena follow. Wetting occurs when the wall preferentially adsorbs one of the phases, say B , while the bulk may be in a different thermodynamic state. At a wetting transition, the thickness $\langle h \rangle$ of the adsorbed B layer diverges. This occurs at all temperatures above a certain wetting temperature, T_w , at bulk phase coexistence, i.e. at $\mu = \mu_c = 0$; by contrast, at $\mu \neq \mu_c$ the thickness of the liquid film may be large, but cannot diverge (bound interface).

Equation (13) is a dynamic model for the relaxation of the interfacial height $h(\mathbf{x}, t)$ towards the equilibrium configuration that minimizes the Hamiltonian

$$\mathcal{H}(h) = \int_0^\infty d\mathbf{x} \left[\frac{\nu}{2} (\nabla h)^2 + V(h) \right] \quad (16)$$

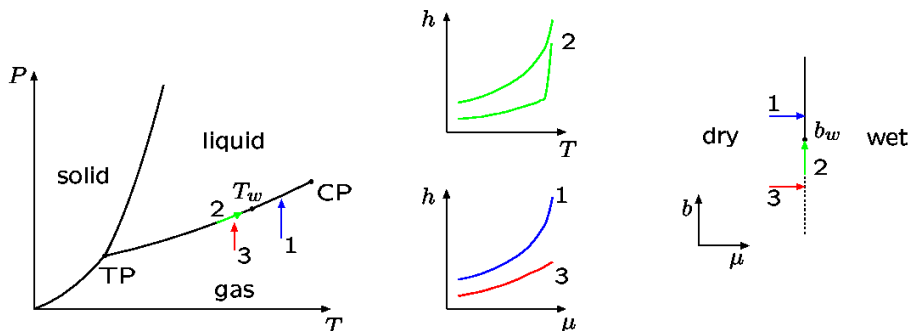


Figure 3: Left, pressure vs. temperature phase diagram of a pure substance. TP , CP and T_w stand for triple point, critical point, and wetting temperature; center, thickness of the wetting layer as a function of the relevant parameters for the paths indicated on the left and on the right; right, phase diagram in the $b - \mu$ plane. Solid and dotted lines correspond to continuous and first-order transitions, respectively (see text).

in the limit $t \rightarrow \infty$. Within mean-field approximation $\langle h \rangle$ follows from the condition $\partial V(h)/\partial h = 0$, whereby one finds that the equilibrium thickness of the wetting layer for an attractive wall ($b < 0$) and long-ranged forces with $m = 3, n = 2$, (non-retarded van der Waals forces [24]) is given by $\langle h \rangle = -2b/3c$. A *critical wetting* transition takes place as $b \sim T - T_w \rightarrow b_w = 0^-$, i.e. the wetting layer thickness diverges as $\langle h \rangle \sim |b - b_w|^{\beta_c}$ with $\beta_c = -1$. This mean-field result was observed experimentally [25] since the upper critical dimension of the long-ranged system is less than three [26].

Critical wetting driven by short-range forces may also occur since the long-ranged interactions can be neglected if the bulk correlation length is sufficiently large i.e., when T_w is close to the bulk T_c . This has been confirmed recently by the observation of effective short-range critical wetting at the liquid-vapor interface of methanol-alkane mixtures [27]. Within mean-field theory, $\langle h \rangle = \ln(-2c/b)$ and, consequently, $\beta_c = 0(\log)$. However, the measured exponents, which are also mean-field like, are at odds with the theoretical, renormalization-group-based predictions [27].

By contrast, the wetting transition may be driven by the chemical potential difference between the A and B phases, at any temperature above T_w ; this is always a continuous transition and it is known as *complete wetting* [23]. A study of complete wetting transitions requires adding a linear term

<i>Exponent</i>	<i>Short-range forces</i>		<i>Long-ranged forces</i>	
	MF	$d < d_c = 2$	MF	$d < d_c(m) = \frac{2m}{2+m}$
$\theta_h, \langle h \rangle \sim t^{\theta_h}$	0	1/4	$1/(2+m)$	$(2-d)/4$
$\nu_x, \xi \sim \delta\mu^{-\nu_x}$	1/2	2/3	$(2+m)/(2+2m)$	$2/(d+2)$
$\beta_h, \langle h \rangle \sim \delta\mu^{-\beta_h}$	0	1/3	$1/(1+m)$	$(2-d)/(d+2)$
$z, \xi \sim t^{1/z}$	2	2	2	2

Table 1: Upper critical dimensions and critical exponents in the mean-field (MF) and the fluctuation regimes for complete wetting transitions with short and long-ranged forces. At the mean-field level, the exponents for short-ranged interactions are recovered in the $m \rightarrow \infty$ limit of the long-ranged ones.

μh to the Hamiltonian, where μ is the chemical potential difference of phases A and B . Thus, on approaching coexistence for $T > T_w$ ($b > 0$ at the mean-field level), $\langle h \rangle$ diverges as $\langle h \rangle \sim |\mu - \mu_c|^{-\beta_h}$, with $\mu_c = 0$, and $\beta_h = 0$ (log) and $\beta_h = 1/(m + 1)$ for short- and long-ranged forces, respectively. Experimental observations of complete wetting transitions are numerous and are characterized, in general, by long-range mean-field exponents (at least far from the bulk critical temperature). The interested reader is referred to [23] for reviews, and to [6] and [28] for a detailed account of recent experimental and Monte Carlo results, respectively.

This rich behavior is summarized in the schematic phase diagram of figure (3): (along path 1) $\langle h \rangle$ diverges continuously as coexistence is approached from the gas phase (complete wetting); (path 2) as T approaches T_w at coexistence $\langle h \rangle$ may diverge either continuously (critical wetting) or discontinuously (first-order wetting); (path 3) the wall remains non wet when coexistence is reached. Clearly, in the wetting regime at long times, the form of $V(h)$, determines the rate of growth that is logarithmic, i.e. $\langle h \rangle \sim t^{\theta_h} \sim \ln t$ or $\theta_h = 0$ for short-ranged interactions and a power law, $\langle h \rangle \sim t^{1/(2+m)}$, for long-ranged repulsive interactions decaying as h^{-m} [20]. Off coexistence, for a small and negative $\delta\mu \equiv \mu - \mu_c$, the wetting layer thickness grows with time as predicted by the mean-field theory, provided that t is much smaller than the correlation time $\delta\mu^{\nu_t}$. Then, it relaxes exponentially to its equilibrium value $\langle h(t = \infty) \rangle$. These exponents are related by $\theta_h = \beta_h/z\nu_x$, and $\nu_t = -2\nu_x$ [20]. On the other hand, if $\delta\mu$ is positive, $\langle h(t) \rangle$ grows linearly.

The results for the exponents are summarized in table (1) and Monte Carlo simulations of the growth of wetting layers can be found in [29, 30].

The behavior below b_w deserves some comments. Wetting only occurs at coexistence. The first-order transition that takes place at $\mu = 0$ has to be distinguished from wetting because it is not driven by the substrate. In fact, the wall is not wet at the transition point and the depinning transition that occurs upon crossing the boundary line $\mu = 0$ is, as such, trivial since to the right of the $\mu = 0$ line liquid is the only stable thermodynamic phase, with or without a wall.

Lastly, we comment briefly on how the effective wall interaction due to fluctuations comes about. As a result of the confinement of the interface, there is an increase in the elastic bending energy and an entropy loss. For $d = 1$ both contributions are of the same order and can be estimated as $\Delta e \approx T\Delta s = \Delta V \sim h^{-2}$, while for $d = 2$ one has $\exp(-2h^2)$ [19]. By simply adding ΔV to $V(h)$ one gets a description of the effects of fluctuations within mean-field theory.

3.2 A bound Kardar-Parisi-Zhang equation

Consider the following dynamic interfacial model

$$\frac{\partial h(\mathbf{x}, t)}{\partial t} = \nu \nabla^2 h + \lambda (\nabla h)^2 + \mu - \frac{\partial V(h)}{\partial h} + \eta(\mathbf{x}, t). \quad (17)$$

The fact that the KPZ equation is not invariant under the transformation $h \rightarrow -h$ implies that the sign of λ assigns an *orientation* to the wall, distinguishing two types: *upper* and *lower* walls. An upper (lower) wall restricts (or even prevents) large interfacial excursions into the region $h > 0$ ($h < 0$). Thus, for negative values of λ the interface is pushed on average against a lower wall, while for positive λ it is pulled away from it, and exactly the opposite occurs at an upper wall. As will be shown below, for a given sign of the non-linearity upper and lower walls lead to quite different phenomenologies, but the case $\lambda > 0$ and a lower wall is completely equivalent to $\lambda < 0$ and an upper wall [31]. We stress that, were it not for the presence of the nonlinear term, such distinctions would not have been necessary (both equilibrium wetting and dewetting are symmetric phenomena).

As noted earlier, in the absence of the limiting wall, bulk coexistence no longer obtains at $\mu = 0$. Rather, a nonzero chemical potential $\mu_c \sim \lambda$ is required to balance the force exerted by the nonlinear term on the tilted

regions of the interface. For $\lambda = 0$ the model reduces to the equilibrium one and $\mu_c = 0$ as usual. As in the previous section, we distinguish the cases of short- and long-ranged interactions. Also, for definiteness, in what follows the wall will always be assumed to be a lower one, while λ may take either sign.

3.2.1 Short-ranged forces

Consider the Langevin equation (17) where $V(h) = be^{-ph} + ce^{-2ph}$. The parameter p controls the nature of the wall: the limit $p \rightarrow \infty$ corresponds to an impenetrable wall and the sign of p determines whether it is an upper (-) or a lower one (+). The same equation with $c = 0$, $b > 0$ (repulsive wall), and $\lambda < 0$ was first studied by Tu *et al.* [32], and by Muñoz and Hwa [31] for arbitrary λ in the context of nonlinear diffusion with multiplicative noise (see later in this article). The effect of inert and attractive walls was then investigated by Hinrichsen *et al.* in [33, 34] using a discrete solid-on-solid model with dynamics that violate detailed balance. The model includes particle adsorption and desorption rates, plus an additional growth rate at the wall that simulates a short-ranged attractive or repulsive interaction between the wall and the interface. Their results were subsequently confirmed and expanded by Giada and Marsili [35] who mapped (17) to a Langevin equation with multiplicative noise and analyzed it within mean-field, and by ourselves [36, 37], by means of direct integration of (17) with $\lambda < 0$. The work of [35] privileges the role of the noise as the driving force, while in [36, 37] the noise strength is fixed and b and μ are taken as control parameters. The case $\lambda > 0$ was recently investigated in [38].

Some of the exponents defined in table (1) may be related to KPZ exponents. In particular, the dynamic exponent z is unchanged from its KPZ value, and $\nu_x = 1/(2z - 2)$ for any value of λ [39, 32]. Thus, in one dimension $\nu_x = 1$ since $z = 3/2$. The two remaining exponents, β_h and θ_h are related by the scaling form $\theta_h = \beta_h/\nu_x z$.

The long-ranged repulsion exerted by the wall on the interface, mentioned previously, may be estimated using a simple scaling argument: the wall makes itself felt when the characteristic distance of the interfacial excursions is of order h , $\xi_\perp \sim h$. From (4) and the definition of ν_x , we find $\xi_\perp \sim \xi^\zeta \sim \delta\mu^{-\nu_x\zeta}$, leading to an effective repulsive force $h^{-1/\nu_x\zeta} \sim h^{-2/\nu_x}$, since $\zeta = 1/2$ in $d = 1$ for both KPZ and EW. By substituting $\nu_x = 2/3$ (see table (1)) we recover the EW result, while $\nu_x = 1$ yields $V(h) \sim h^{-1}$ for the KPZ [31].

$\lambda < 0$. We first consider a negative KPZ non-linearity. Before discussing the results, we note that upon inverting the sign of h , λ changes to $-\lambda$ and p to $-p$, so that the exponential now acts as an upper wall and $\lambda > 0$ pushes the interface against it. This shows that the cases $\lambda > 0$ —upper-wall and $\lambda < 0$ —lower-wall are equivalent.

The associated phase diagram in the $b - \mu$ plane is depicted in figure (4). The solid line is the continuous phase boundary between depinned and pinned phases. Between the dashed lines, both of which correspond to first-order boundaries, the pinned and depinned phases coexist as stationary solutions of the dynamical equation. The three lines meet at the tricritical point (μ_c, b_w) .

The unbinding transition at $\mu = \mu_c$ for any $b > b_w$ is the analogue of the equilibrium complete wetting phase transition (path 1 of fig. (4)). The exponent governing the divergence of $\langle h \rangle$ is $\beta_h \approx 0.41$, with error bars that exclude the equilibrium value $\beta_h = 1/3$ [33, 40]. Along path 2, which corresponds to a nonequilibrium critical wetting transition, b is progressively increased until the nonwet phase becomes unstable at b_w . It is found that the critical temperature is depressed from its mean-field value $b_w = 0$, with an associated critical exponent $\beta_c \approx -1.2$ [37].

As for the behavior below b_w (attractive wall) there are two first-order depinning transitions by varying μ (paths 3 and 4 of figure (4)). Recall that, if the wetting temperature is to be a meaningful concept, the depinning transition for $b < b_w$ cannot be viewed as a wetting transition or, in other words, these transitions occur not on approaching coexistence, but when *crossing* the boundary line. For sufficiently negative values of b the pinned phase becomes unstable at $\mu^*(b)$ (path 4), and the depinned phase at $\mu_c < \mu^*(b)$ (path 3). Consequently, in the range $\mu_c < \mu < \mu^*(b)$ both phases coexist in the sense that if the interface is initially close to the wall it remains pinned, while if it is initially far from the wall it detaches and moves away at a constant velocity. As a consequence of the “broad” phase boundary there is the possibility of defining critical wetting along a range of different paths, delimited by the dashed lines of figure (4). It has been checked that the exponent β_c does not change when the tricritical point is approached along different paths within this region [37].

The fact that the coexistence region is finite rather than a line is a nonequilibrium effect since at equilibrium two-phase coexistence only occurs on a surface of dimension one less than the dimension of the space of thermodynamic parameters. An equilibrium system initially in a state other than the equilibrium one will be destabilized by local fluctuations in the form

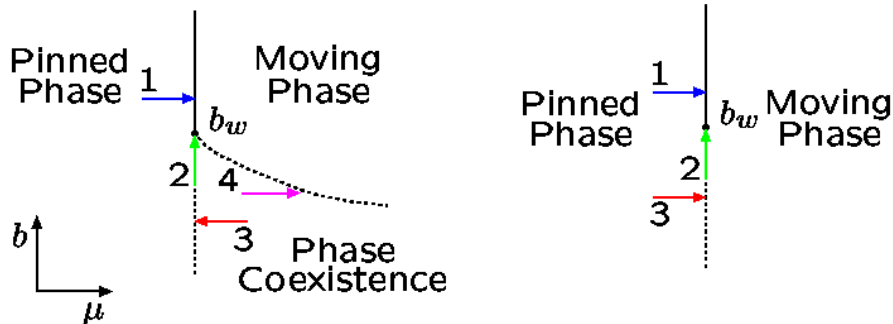


Figure 4: Phase diagrams for $\lambda < 0$ (left) from numerical solutions of (17) in short-ranged potentials, and $\lambda > 0$ (right) from discrete models. The arrows denote different types of transitions explained in the text.

of droplets of the equilibrium phase. To ensure generic multistability, a robust mechanism for eliminating these droplets of the minority phase must exist. In the present case, such a mechanism was found by Hinrichsen *et al.* [34]: when, due to thermal fluctuations, a segment of the interface overcomes the potential barrier and gets out of the potential well (see figure (2)), it rapidly acquires a triangular shape, after which it shrinks at a constant velocity driven by the negative nonlinear term, in a time proportional to its size. Typical interface profiles resulting from numerical solutions of (17) in $d = 1$ and 2 are shown in figure (5) (similar configurations are described in the discrete model of reference [34]). The largest size of the depinned regions, i.e. the size of the triangular bases, increases as the instability threshold μ^* is approached. Once the last site has detached, the interface “takes off” and a transition from a pinned to a moving phase takes place. In fact, owing to finite-size effects the only stable phase within the coexistence region is the moving one, making the analysis of the pinned regime rather hard. This difficulty is circumvented by studying τ , the time taken by the interface to depin in the limit $L \rightarrow \infty$. For $\mu > \mu^*$, τ saturates with increasing system-size and thus the interface detaches in a finite time. For $\mu_c < \mu < \mu^*$, however, τ grows exponentially with the system-size so that the pinned phase becomes stable in the thermodynamic limit. The stationary distribution of triangles as a function of their base-size turns out to be exponential. This indicates that there is a typical size for the depinned regions and rules out the possibility that growth is driven by a coarsening mechanism [37]. Another interesting

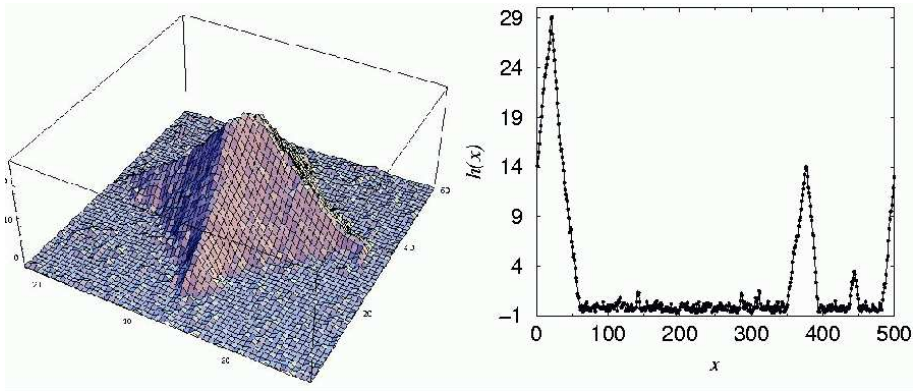


Figure 5: Snapshots of $d = 2, 1$ interfacial configurations within the coexistence region, from numerical solutions of (17) in a short-ranged potential.

feature is that, for a given pair of parameters μ and b , all the triangular facets have the same slope, s , which can be determined through the relation $|\lambda_R|s^2 = \mu$, where λ_R is the renormalized nonlinear coefficient of the KPZ. Historically, the possibility of a finite phase boundary was first discussed in Toom’s north-east-center voter model [41]. Other examples include systems of harmonically-coupled, identical nonlinear constituents under the simultaneous influence of additive and multiplicative noise [42], and a Leshhorn automaton subject to transient velocity-dependent forces [43].

It has been pointed out that upon diminishing both the depth of the potential well and the surface tension, the first-order phase transition at μ^* becomes continuous with *directed percolation* (DP) critical exponents [44].³ This is in line with a recent claim that first-order phase transitions in one-dimensional nonequilibrium systems with fluctuating ordered phases are impossible, provided there are no conservation laws, long-ranged interactions, macroscopic currents, or special boundary conditions [45]. If this is the case, the reported first-order behavior will be a very long transient effect. The presence of DP behavior is now a well-established result that was found in a variety of discrete models [44, 46, 47]. Nevertheless, we cannot discard the presence of a tricritical point for sufficiently negative values of b , separating DP from first-order transitions. At present, this question remains open.

³To observe DP behavior a different order-parameter, namely the density of pinned sites, has to be used. More on this later

$\lambda > 0$. Consider $\lambda > 0$. Early results were reported in [31], but the observed critical exponents are far from their true asymptotic values. Later studies revealed marked differences when compared to the system with a negative nonlinearity and attractive walls [34, 38]. These are apparent in the phase diagram of figure (4), similar to that of $\lambda = 0$ (figure (3)). Before we proceed, we note that the results of this section were obtained using Monte Carlo simulations of discrete models. Attempts at numerical integration of a bound KPZ equation failed to reach a stationary state. It is well known that the results from numerical integration may disagree with the predictions from the continuum KPZ [48]. The usual way to handle the integration of the KPZ equation with short-ranged forces and negative nonlinearity, the Cole-Hopf transformation, is also plagued with instabilities. Furthermore, mean-field approaches also fail to predict the correct phase diagram [38].

We start by describing the results for a repulsive wall. A continuous wetting transition is found as $\mu \rightarrow \mu_c$ when $b > b_w$ ($b_w = 0$ at the mean-field level; path 1 of figure (4)). The behavior of the order parameter in the vicinity of the critical point yields $\beta_h = 0.52(2)$, and the time evolution of $\langle h \rangle$ at μ_c behaves as $\langle h(t) \rangle \sim t^{\theta_h}$, with $\theta_h = 0.355(15)$ [38]. From the scaling relation $z = \beta_h/\nu_x\theta_h$, $z = 0.52(2)/0.355(15) = 1.5(1)$ in good agreement with the theoretical prediction $z = 3/2$. These results, however, disagree with those of reference [33] probably due to the presence of extremely long transients in the latter. The results are collected in table (2).

For attractive walls, we note that there is a line of first-order depinning transitions ending at a tricritical point at b_w (path 3 of figure (4)). By contrast to what happens for $\lambda < 0$, phase-coexistence is restricted to a line since the mechanism responsible for the elimination of droplets of the depinned phase works only for negative λ . Finally, the tricritical behavior associated with the transition along path 2 has not been investigated yet.

3.2.2 Long-ranged forces

Next, consider the KPZ equation in the presence of a long-ranged potential $V(h) = b(T)h^{-m} + ch^{-n}$. The resulting equation is not amenable to analytical treatment and therefore we are limited to numerical results from Monte Carlo simulations of one-dimensional, discrete models. Recently, Lipowski and Droz [46] studied an interfacial growth model with dynamics inspired by the synchronization transition in coupled map lattices and included a power-

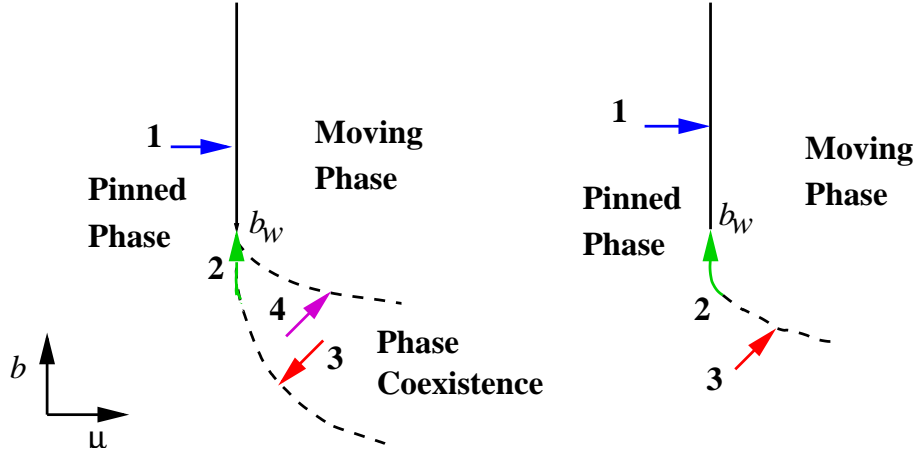


Figure 6: Phase diagram for long-ranged potentials. Left, $\lambda < 0$; right, $\lambda > 0$.

law interaction between the interface and the wall.⁴ The model, however, lacks a surface tension and its microscopic rules are such that it is difficult to ascertain whether it may be described by a bound KPZ equation.

Interestingly enough, the KPZ nonlinearity appears to be irrelevant above the wetting temperature b_w for any sign of λ , and an equilibrium complete-wetting transition is found along paths 1 of figure (6) [49]. The associated exponents are collected in table (1) and have been verified numerically in a simulation of a variant of a model introduced in [16], whose continuum counterpart is known to be the KPZ with $\lambda < 0$ and a lower wall [50].

$\lambda < 0$. Below b_w , a phase diagram similar to that for short-ranged interactions is found (Fig. (6), left), the main difference being that μ_c becomes temperature-dependent (path 3). For the set of parameters explored, the transition at $\mu^*(b)$ (path 4) is characterized by DP exponents when the order parameter $n = \exp(-h)$ is used [50].

$\lambda > 0$. To our knowledge, there are no published results on this case. Preliminary results of ours seem to indicate a phase diagram similar to the one shown on the right of figure (6): along path 3 the system undergoes a discontinuous transition. The analogue to a nonequilibrium critical/first-order wetting transition along path 2 has not been investigated.

⁴The relationship between synchronization transitions and a bound KPZ will be seen in the next section.

4 Related phenomena

In this section, the directed-polymer representation of the KPZ is exploited to analyze bound KPZ interfaces. As shown in section 2.2, the KPZ can be linearized by means of the Cole-Hopf transformation, $n(\mathbf{x}, t) = \exp[\alpha h(\mathbf{x}, t)]$, at the cost of introducing a multiplicative-noise (MN) term. This transforms the KPZ equation (8) into

$$\frac{\partial n(\mathbf{x}, t)}{\partial t} = \nu \nabla^2 n + n\eta. \quad (12)$$

Note that the noise amplitude vanishes for $n = 0$, and neither the deterministic dynamics, nor fluctuations can take the system out of this state. For this reason the configuration $n = 0$ is known in the MN literature as an *absorbing* state, while $n \neq 0$ is commonly referred to as the *active* phase. This representation has been successfully applied to the case of short-range interactions with a negative non-linearity, enabling analytic calculations both at the mean-field level [35, 36, 37, 42], and beyond via a renormalization group approach [32, 39]. Let us consider again (17) in the presence of a short-ranged potential with, for simplicity, $-\lambda = \nu = D = 1$ (different coefficients for the Laplacian and the KPZ nonlinearity may be accounted for by a proper choice of α). The change of variables $h = -\ln n$ leads to

$$\frac{\partial n(\mathbf{x}, t)}{\partial t} = \nu \nabla^2 n - \frac{\partial V(n)}{\partial n} + n\eta, \quad (18)$$

with $V(n) = \mu n^2/2 + bn^3/3 + cn^4/2$, and where we have made use of the Stratonovich calculus [51, 52].⁵ In general, potentials of the form $V(n) = bn^{p+2} + cn^{2p+2}$ with $p > 0$ result in equivalent effective Hamiltonians since, when expressed in terms of h , p can be eliminated by defining the length scale. In the n language, unbinding from the wall, $\langle h \rangle \rightarrow \infty$, corresponds to a transition to an absorbing state, $\langle n \rangle \rightarrow 0$, recovering the usual behavior of Landau theory where the order parameter becomes small rather than large near the transition.⁶ To complete the analogy between the MN and the interfacial descriptions, one can give a physical interpretation to n by noting that it is the density of sites at zero height, $n(\mathbf{x}, t) = \delta_{h(\mathbf{x}, t), 0}$ [53]. The

⁵The difference between the Ito or the Stratonovich results is a trivial shift in μ .

⁶Strictly speaking, at unbinding the system is in a state that evolves continuously to the absorbing state.

behavior of $\langle n \rangle$ is characterized by a set of exponents similar to that of $\langle h \rangle$: $\langle n \rangle \sim t^{-\theta_n}$, $\langle n \rangle \sim \delta\mu^{\beta_n}$, $\xi \sim \delta\mu^{-\nu_x}$, and $\xi \sim t^{1/z}$. Some of these exponents are obtained from the KPZ exponents using scaling arguments. For instance, it was shown in [32, 39] that the dynamic exponent for the MN case is identical to the value of the KPZ z , that ν_x is related to it through $\nu_x = 1/(2z-2)$, and that $\beta_n > 1$. Also, the scaling relation $\theta_n = \beta_n/\nu_x z$ is satisfied. It is therefore not surprising that the phase diagram of the MN equation (18) is very similar to that of the KPZ. There is a strong noise phase for $d \leq d_c = 2$, and both a weak and a strong noise phases for $d > 2$ depending on the noise intensity D . Weak and strong phases obtain for values of D that are, respectively, smaller and larger than a critical value [32]. See [54] for a comparative list of critical indices below and above d_c .

In this context, (18) is a Langevin-like equation for a reaction-diffusion process where n is a coarse-grained particle density. Indeed, it has been argued in [55] that (18) is the equation governing the pair contact process with diffusion, $2A \rightarrow 3A$, $2A \rightarrow \emptyset$, the critical behavior of which is currently under debate (see [53] and references therein). A different realization of (18) comes from the field of synchronization in spatially extended systems. Pikovsky *et al.* [56] established that the difference field, $n(\mathbf{x}, t)$, between two coupled-map lattices follows (18) with $c = 0$. Two replicas of a coupled-map lattice are synchronized when $n = 0$, $n \neq 0$ corresponding to the asynchronous regime, and the active-absorbing, or the pinning-depinning, phase transition is analogous to a synchronization transition. As a last example, (18) has been studied in [57] in the context of spatio-temporal intermittency. The unsuspected connections between these problems are illustrated in what follows.

The mean-field approximation to (18) consists of discretizing the Laplacian as $1/2d \sum_j (n_j - n_i)$, where $n_i = n(x_i, t)$ and the sum is over the nearest-neighbors of i . Substituting the values of the nearest-neighbors by the average field, $\langle n \rangle$, a closed Fokker-Planck equation is obtained for $P(n, t, \langle n \rangle)$. This approach takes into account the effect of the noise and of a spatially varying order parameter. The steady-state solution is then found from the self-consistency requirement

$$\langle n \rangle = \frac{\int_0^\infty dn n P(n, \langle n \rangle)}{\int_0^\infty dn P(n, \langle n \rangle)}, \quad (19)$$

resulting in a phase diagram equivalent to that of figure (4) with a tricritical point at $(\mu = 0, b_w = 0)$ [36, 37]. Thus, for repulsive walls a complete wetting

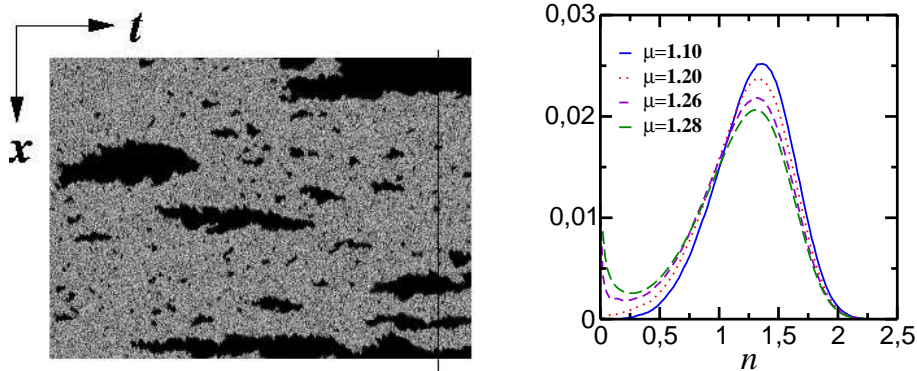


Figure 7: Left, spatio-temporal evolution from a numerical solution of (18) within the coexistence region. Depinned regions ($n < 1$) are colored in dark gray and pinned ones ($n > 1$) in light gray. The instantaneous interfacial configuration for the time marked by the line is shown in figure (5). Right, single-site probability density function for different values of μ , also within the coexistence region. The stability edge is $\mu^*(b = -4) \approx 1.3$.

transition characterized by $z = 2$, $\nu_x = 1/2$, and $\theta_n = 1$, is found at $\mu_c = 0$ for any $b > 0$. Different mean-field approaches yield different results for the exponent β_n , namely $1/p$ [54] and $D/2$ [35], but this has been clarified in [58] where a crossover from $1/p$ to a nonuniversal, continuous exponent $D/2\nu$ was identified. For attractive walls, the three regimes previously described are recovered, namely, an active phase for $\mu < \mu_c = 0$, an absorbing one for $\mu > \mu^*(b)$, and phase coexistence of the active and absorbing phases in the region $0 < \mu < \mu^*(b)$. A qualitatively equivalent picture is obtained using a different space of parameters, for instance the strength of the noise vs. μ [35].

Beyond mean-field theory, (18) is known to be superrenormalizable above $b = 0$, i.e. the Feynman graphs may be computed to all orders and resummed [32, 39]. This does not imply that all the critical exponents are given, as the renormalization group-flow equation has runaway trajectories that are supposed to converge to the strong coupling fixed point. Representative results for $d = 1$ are summarized in table (2).

The rich phenomenology obtained for attractive walls is also observed within the MN framework. Active and absorbing phases coexist over a finite area $\mu_c < \mu < \mu^*(b)$, and lose their stability at, $\mu^*(b)$ and μ_c , respectively.

<i>Exponent</i>	$\lambda < 0$		$\lambda > 0$		DP [59]
	<i>h</i> [40]	<i>n</i> [54]	<i>h</i> [38]	<i>n</i> [38]	
$\theta_{h,n}$	—	1.1(1)	0.355(15)	0.215(15)	0.1594
ν_x	—	1.0(1)	—	0.97(5)	1.7338
$\beta_{h,n}$	0.41	1.5(1)	0.52(2)	0.32(2)	0.2765
<i>z</i>	—	1.52(3)	—	1.55(5)	1.5807

Table 2: Summary of the universality classes discussed in the text for short-ranged forces. For transitions other than DP, the theoretical predictions are $z = 3/2$, $\nu_x = 1$, and $\beta_n > 1$ if $\lambda < 0$.

The phase-coexistence regime may be characterized by analyzing the single-site stationary density function, defined as the average of $n(t)$ over pinned states rather than over all runs. This is depicted in figure (7) and shows how the histogram develops a maximum at $n = 0$ as μ approaches the stability edge $\mu^*(b)$, beyond which it changes abruptly into a delta function and the pinned phase becomes unstable. The simultaneous presence of two-peaks indicates that a fraction of the interface depins. This is clearly seen in the space-time snapshot of a numerical solution of (18), on the left of figure (7). The main features of such a pattern, spontaneous formation of domains with a wide range of sizes and lifetimes, has been identified as distinctive of spatio-temporal intermittency [57].

Numerical simulations provide evidence of a first-order phase transition at μ_c . As was pointed out previously, both first-order and continuous transitions are observed at $\mu^*(b)$ depending on the model parameters. For instance, a continuous DP-like transition was recently reported in [44] as the numerical solution of (18) with $b = -9$, $c = 8$, $\nu = 0.1$, and $D = 1$. By contrast, for $b = -3$, $c = 2$, $\nu = D = 1$, a first-order transition was found. The minimal Langevin equation that describes the DP universality class is

$$\frac{\partial n(\mathbf{x}, t)}{\partial t} = \nu \nabla^2 n - \mu n - bn^2 + \sqrt{n}\eta, \quad (20)$$

which differs from (18) by the $n^{1/2}$ noise amplitude. Thus, it appears that DP-like noise takes over the MN-noise, proportional to the field n , as the wall changes from repulsive to attractive in a given range of parameters. Deriving (20) from (18) is an interesting theoretical problem that remains open.

A direct application of the Cole-Hopf transformation $n = \exp(-h)$ to (17) with $\lambda > 0$ in the presence of short-ranged interactions yields the Langevin equation

$$\frac{\partial n(\mathbf{x}, t)}{\partial t} = \nu \nabla^2 n - 2 \frac{(\nabla n)^2}{n} - \mu n - bn^2 - 2cn^3 + n\eta, \quad (21)$$

which is (18) plus the extra term $-2(\nabla n)^2/n$. Apart from the factor -2, equation (21) is the Cole-Hopf transform of

$$\frac{\partial h}{\partial t} = \nabla^2 h + \mu + be^{-h} + ce^{-2h} + \eta \quad (22)$$

which is the equilibrium EW model in the presence of a binding wall. Note that the factor of 2 in (21) cannot be absorbed by reparametrization. Indeed, equation (21) does not admit proper mean-field solutions, it is not amenable to standard perturbative field theoretical methods, and cannot be integrated numerically [38]. Nevertheless, (21) may be studied within the framework of active/absorbing phase transitions by simulating discrete growth models, and monitoring the order parameter $n = \exp(-h)$. This was done in [38] for two different models argued to correspond to a bound KPZ with $\lambda > 0$ and short-ranged interactions. Results suggest the existence of a new universality class characterized by $\beta_n = 0.33, \theta_n \approx 0.22, z = 1.5, \nu_x \approx 1$. For a sufficiently attractive wall, the transition becomes first-order.

h or n? The Cole-Hopf transform puts the problem of bound KPZ interfaces in a rather different context. For $\lambda < 0$, a more compact equation, instability-free and amenable to a mean-field analysis, is obtained, whereas for $\lambda > 0$ the presence of $(\nabla n)^2/n$ suggests that the interface language is most natural. We stress, however, that the form of the continuum equation does not determine the “correct” order-parameter: In fact, proper scaling behavior is found for both h and n in discrete models. DP is a counterexample since the interface representation of the contact process shows clear signs of anomalous scaling [60]. Another interesting point concerns the n -representation of the EW problem, that is, the equilibrium limit ($\lambda = 0$) of (17). The Cole-Hopf transform fixes the ratio λ/ν and thus the $\lambda = 0$ limit cannot be taken when the transformation is used. A comparison of published results on equilibrium and nonequilibrium wetting, reveals that the EW plus a wetting potential is not equivalent to the KPZ in the weak-coupling regime plus the same wetting potential.

5 Experimental realizations

Since the idea of a wetting transition was introduced in 1977 by Cahn [61], much experimental effort has gone into its realization, ultimately awarded by the confirmation of a large number of theoretical predictions. The obvious question then arises of what are the experimental realizations of the phenomenology described for the bound KPZ interface. As was discussed in section 2.2, the KPZ non-linearity models lateral growth. Although this mechanism is unlikely to be relevant in simple fluids, it may be important in describing systems with anisotropic interactions for which the growth of tilted interfaces depends on their orientation. For instance, it has been shown that crystal growth from atomic beams when desorption is allowed is described by the KPZ equation [62]. Furthermore, a renormalization group analysis reveals that the KPZ term is always generated, except when excluded by symmetry, whenever elastic objects depin in the presence of anisotropy [63]. This suggests that an answer may come from the field of crystal growth. Crystals grown by deposition of material onto a crystal substrate from a vapor phase can display wetting behavior. At sufficiently low temperatures, the adsorbate that intervenes between the substrate and the vapor may form small crystallites, which melt upon increasing the temperature, leading to the formation of liquid droplets. On approaching the wetting temperature, the liquid spreads over the substrate and coats it uniformly. Growth of solid phases is also possible, but in this case the wetting layer is likely to be under stress due to the misfit between the lattice constants of the substrate and the adsorbate. Two well-known relaxing mechanisms are the formation of misfit dislocations and the deformation of the surface (Asaro-Tiller-Grinfeld instability [64]). Faceting and, in particular, the appearance of pyramidal structures similar to those of figure (7) have been reported in simulations of wetting-layers and island formation in heteroepitaxial growth [65]. These structures can either form directly on the substrate (Vollmer-Weber growth) or on top of a wetting-layer of finite thickness (Stranski-Krastanov-like growth). Clearly, further work is needed before a connection between crystal growth and a bound KPZ can be substantiated.

A second direction of research is the experimental verification of synchronization transitions in extended, one-dimensional systems. The order parameter for such transitions is the difference between two dynamical systems coupled to each other, $n(x, t) = |u_1(x, t) - u_2(x, t)|$. Starting from different initial conditions, the systems become synchronized in the stationary

limit, $\langle n \rangle = 0$, above a certain critical coupling strength, and asynchronized, $\langle n \rangle > 0$, otherwise. The character of the transition depends on whether the largest Lyapunov exponent of the system, Λ , is zero or negative. In the former case, the transition is in the MN universality class, while in the latter it is DP-like or discontinuous depending on the system details. Equation (18) is a stochastic model for the difference field n , with $\Lambda = \mu_c$ at the transition. Examples of such chaotic coupled-systems include semiconductor laser arrays and liquid crystals describable by the anisotropic Ginzburg-Landau equation, for which the aforementioned behavior should be experimentally detectable [66, 67]. This goes hand in hand with finding a system which reproduces the critical exponents of directed percolation, a problem that so far has defied all attempts of solution despite extensive empirical efforts [68].

The other large class of bound KPZ —short-ranged forces, positive non-linearity, and a lower wall— should also describe actual nonequilibrium wetting phenomena. There is nonetheless one other possible experimental realization. Sequence alignment is a powerful tool for determining relatedness between sequences of proteins or DNA segments. Algorithms have been devised to detect such correlations, the Smith-Waterman being among the most sensitive for finding related sequences in a database [69]. Scores are assigned to each character-to-character comparison: positive for exact matches and negative if the two are different, or if pairing of an element with a gap occurs. An optimal alignment is one with the maximum possible score. Recently, Hwa *et al.* have mapped this algorithm to a KPZ with a lower wall, where the location of the critical point corresponds to the choice of the optimal scoring parameters [70].

Acknowledgements. We are grateful to M.A. Muñoz for a critical reading of the manuscript.

References

- [1] A.-L. Barabási and H.E. Stanley, *Fractal Concepts in Surface Growth*, Cambridge University Press, Cambridge (1995), and references therein.
- [2] P. Meakin, *Fractals, Scaling, and Growth far from Equilibrium*, Cambridge University Press, Cambridge (1998).
- [3] D. Jasnow, Rep. Prog. Phys. **47**, 1059 (1984).

- [4] T. Halpin-Healy and Y.-C. Zhang, Phys. Rep. **254**, 215 (1995), and references therein.
- [5] P.J. Upton, Phys. Rev. E **60**, R3475 (1999).
- [6] D. Bonn and D. Ross, Rep. Prog. Phys. **64**, 1085 (2001).
- [7] M.A. Muñoz, to appear in *Advances in Condensed Matter and Statistical Mechanics*, Ed. E. Korutcheva and R. Cuerno, Nova Science Publishers; cond-mat/0303650.
- [8] S.F. Edwards and D.R. Wilkinson, Proc. R. Soc. London A **381**, 17 (1982).
- [9] F. Family and T. Vicsek, J. Phys. A **18**, L75 (1985).
- [10] A. Maritan, F. Toigo, J. Koplik, and J.R. Banavar, Phys. Rev. Lett. **69**, 3193 (1992).
- [11] M. Kardar, G. Parisi and Y. C. Zhang, Phys. Rev. Lett. **56**, 889 (1986).
- [12] I. Pagonabarraga and J. M. Rubí, Phys. Rev. Lett. **74**, 114 (1994); P. Wojtaszczyk and J. B. Avalos, Phys. Rev. Lett. **80**, 754 (1998).
- [13] R. Cuerno and M. Castro, Phys. Rev. Lett. **87**, 236103 (2001).
- [14] J. Krug, Phys. Rev. A **36**, 5465 (1987).
- [15] S.V. Ghaisas, cond-mat/0307411.
- [16] J. Krug, Adv. Phys. **46**, 139 (1997); J. Krug and H. Spohn, in *Solids far from equilibrium*, Ed. C. Godrèche, Cambridge University Press (1991).
- [17] J. Krug and P. Meakin, J. Phys. A **23**, L987 (1990).
- [18] R. Bausch, V. Dohm, H.K. Janssen, and R.K.P. Zia, Phys. Rev. Lett. **47**, 1837 (1981).
- [19] R. Lipowsky and M.E. Fisher, Phys. Rev. B **36**, 2126 (1987).
- [20] R. Lipowsky, J. Phys. A **18**, L585 (1985).
- [21] M. Grant, Phys. Rev. B **37**, 5705 (1988).

- [22] E. Brézin, B.I. Halperin, and S. Leibler, *J. Phys. (Paris)* **44**, 775 (1983).
- [23] S. Dietrich, in *Phase Transitions and Critical Phenomena*, vol. 12, edited by C. Domb and J. Lebowitz, Academic Press (1983); D.E. Sullivan and M.M. Telo da Gama, in *Fluid Interfacial Phenomena*, ed. C.A. Croxton. Wiley, New York (1986).
- [24] I.E. Dzyaloshinskii, E.M. Lifshitz, and L.P. Pitaevskii, *Adv. Phys.* **10**, 165 (1961).
- [25] K. Ragil, J. Meunier, D. Broseta, J.O. Indekeu, and D. Bonn, *Phys. Rev. Lett.* **77**, 1532 (1996).
- [26] R. Lipowsky, *Phys. Rev. Lett.* **52**, 1429 (1984).
- [27] D. Ross, D. Bonn, and J. Meunier, *Nature* **400**, 737 (1999).
- [28] K. Binder, D.P. Landau, and M. Müller, *J. Stat. Phys.* **110**, 1411 (2003).
- [29] K.K. Mon, K. Binder, and D.P. Landau, *Phys. Rev. B* **35**, 3683 (1987).
- [30] Z. Jiang and C. Ebner, *Phys. Rev. B* **36**, 6976 (1987).
- [31] M.A. Muñoz and T. Hwa, *Europhys. Lett.* **41**, 147 (1998).
- [32] Y. Tu, G. Grinstein and M.A. Muñoz, *Phys. Rev. Lett.* **78**, 274 (1997).
- [33] H. Hinrichsen, R. Livi, D. Mukamel, and A. Politi, *Phys. Rev. Lett.* **79**, 2710 (1997).
- [34] H. Hinrichsen, R. Livi, D. Mukamel, and A. Politi, *Phys. Rev. E* **61**, R1032 (2000).
- [35] L. Giada and M. Marsili, *Phys. Rev. E* **62**, 6015 (2000).
- [36] F. de los Santos, M.M. Telo da Gama, and M.A. Muñoz, *Europhys. Lett.* **57**, 803 (2002).
- [37] F. de los Santos, M.M. Telo da Gama, and M.A. Muñoz, *Phys. Rev. E* **67**, 021607 (2003).
- [38] M.A. Muñoz, F. de los Santos, and A. Achahbar, *Braz. J. Phys.* **33**, 443 (2003).

- [39] G. Grinstein, M.A. Muñoz, and Y. Tu, Phys. Rev. Lett. **76**, 4376 (1996).
- [40] F. de los Santos, M.M. Telo da Gama, and M.A. Muñoz, Proceedings of the 7th Granada Seminar on Computational Physics. Ed. J. Marro and P. L. Garrido; Am. Inst. Phys. 661 (2003).
- [41] A.L. Toom, in *Multicomponent Random Systems*, edited by R.L. Dobrushin, Marcel Dekker, New York (1980); see also C.H. Bennett and G. Grinstein, Phys. Rev. Lett. **55**, 657 (1985).
- [42] R. Müller, K. Lippert, A. Künel, and U. Behn, Phys. Rev. E **56**, 2658 (1997).
- [43] R. Maimon and J.M. Schwarz, cond-mat/0301495.
- [44] M.A. Muñoz and R. Pastor Satorras, Phys. Rev. Lett. **90**, 204101 (2003).
- [45] H. Hinrichsen, cond-mat/0006212.
- [46] A. Lipowski and M. Droz, Phys. Rev. E **68**, 056119 (2003).
- [47] F. Ginelli, V. Ahlers, R. Livi, A. Pikovsky, A. Politi, and A. Torcini, Phys. Rev. E **68**, 065102 (2003).
- [48] T. J. Newman and A. J. Bray, J. Phys. A **29**, 7917 (1996); C.H. Lam and F. G. Shin, Phys. Rev. E **58**, 5592 (1998).
- [49] R. Lipowsky, in *Random Fluctuations and Pattern Growth*, edited by H. Stanley and N. Ostrowsky, Nato ASI Series E, vol 157, Kluwer Akad. Publ., Dordrech (1988).
- [50] F. de los Santos *et al.*, in preparation.
- [51] N.G. van Kampen, *Stochastic Processes in Physics and Chemistry*, North Holland (1992).
- [52] C.W. Gardiner, *Handbook of Stochastic Methods*, Springer Verlag, Berlin and Heidelberg (1985).
- [53] H. Hinrichsen, cond-mat/0302381.
- [54] W. Genovese and M.A. Muñoz, Phys. Rev. E **60**, 69 (1999).

- [55] M.J. Howard and U.C. Täuber, J. Phys. A, **30**, 7721 (1997).
- [56] A.S. Pikovsky and J. Kurths, Phys. Rev. E **49**, 898 (1994); V. Ahlers and A.S. Pikovsky, Phys. Rev. Lett. **88**, 254101 (2002).
- [57] M.G. Zimmermann, R. Toral, O. Piro, and M. San Miguel, Phys. Rev. Lett. **85**, 3612 (2000).
- [58] T. Birner, K. Lippert, R. Müller, A. Künel, and U. Behn, Phys. Rev. E **65**, 046110 (2002).
- [59] I. Jensen, J. Phys. A **32**, 5233 (1999).
- [60] R. Dickman and M.A. Muñoz, Phys. Rev. E **62**, 7632 (2000).
- [61] J. Cahn, J. Chem. Phys. **66**, 3667 (1977).
- [62] J. Villain, J. Phys. I, **19**, 1 (1991); A. Pimpinelli and J. Villain, *The Physics of Crystal Growth*, Cambridge University Press, New York (1998).
- [63] P. Le Doussal and K.J. Wiese, Phys. Rev. E **67** 016121 (2003).
- [64] P. Politi, G. Grenet, A. Marty, A. Ponchet, and J. Villain, Phys. Rep. **324**, 271 (2000).
- [65] F. Munch and M. Biehl, Europhys. Lett. **63**, 14 (2003).
- [66] A. Pikovsky, M. Roseblum, and J. Kurths, *Synchronization: a universal concept in nonlinear sciences*, vol. 12 of Cambridge Nonlinear Science Series, Cambridge University Press, Cambridge (2001).
- [67] V. Ahlers, Ph.D. Thesis, <http://www.volkerahlers.de/publications.html>.
- [68] H. Hinrichsen, Braz. J. Phys **30**, 69 (2000); Adv. Phys. **49**, 815 (2000).
- [69] T.F. Smith and M.S. Waterman, J. Mol. Biol. **147**, 195 (1981).
- [70] T. Hwa and M. Lassig, Phys. Rev. Lett. **76**, 2591 (1996); see also, T. Hwa and M. Lassig, “Optimal Detection of Sequence Similarity by Local Alignment” in Proceedings of the Second Annual Int. Conf. on Computational Molecular Biology (RECOMB98), S. Istrail, P. Pevzner, and M.S. Waterman eds., 109-116 ACM Press (1998).